Reducing Mixed Noise from Hyperspectral Images

Hemant Kumar Aggarwal, *Student Member, IEEE,* Angshul Majumdar, *Member, IEEE*

***Abstract*—This letter introduces a hyperspectral denoising algorithm based on spatio-spectral total variation. The denoising problem has been formulated as a mixed noise reduction problem. A general noise model has been considered which accounts for not only Gaussian noise but also sparse noise. Inherent structure of hyperspectral images has been exploited by utilizing 2D-total variation along spatial dimension and 1D-total variation along spectral dimension. The denoising problem has been formulated as an optimization problem whose solution has been derived using the split-Bregman approach. Experimental results demonstrates that proposed algorithm is able to reduce significant amount of noise from real noisy hyperspectral images. The proposed algorithm has been compared with existing state-of-the-art approaches. The quantitative and qualitative results demonstrate the superiority of proposed algorithm in terms of peak signal to noise ratio, structural similarity and the visual quality.**

***Index Terms*—Spatio-Spectral Total Variation, Split-Bregman, Hyperspectral Denoising.**

I. Introduction

IMAGES captured over hundreds of bands of electromagnetic spectra ranging from around 400 nm to 2500 nm are generally termed as hyperspectral images. These images are useful in various application domains such as agriculture, forensics, resource management, environmental monitoring etc. Most of the applications require denoising as a pre-processing step.

Images are corrupted by noise due to several reasons including fluctuations in power supply, dark current, non-uniformity of detector response etc. A real hyperspectral image may get corrupted by several kinds of noise including Gaussian noise, random valued impulse noise, salt-and-pepper noise, horizontal and vertical deadlines etc. Therefore hyperspectral denoising is a mixed noise reduction problem consisting of a mixture of Gaussian noise and sparse noise. The term sparse noise [1] refers to the noise which corrupts only few pixels in the image but corrupts them heavily. The sparse noise includes random valued impulse noise, salt-and-pepper noise, horizontal and vertical dead-lines. The line stripping problem mostly occurs when sensors goes out of radiometric calibration.

In this work, we propose to reduce mixed Gaussian and sparse noise from hyperspectral images by explicitly considering them in the proposed problem formulation. Hyperspectral denoising is a well studied problem [2]–[7]. There are studies such as [8]–[10] which consider mixed noise reduction from gray scale images. These studies consider mixture of only Gaussian and salt-and-pepper noise whereas we address a realistic scenario by taking into account more general noise and attempt to solve this problem for hyperspectral images. A recent low-rank matrix recovery (LRMR) based denoising approach [1] can reduce mixed noise from hyperspectral images. The low-rank based model is a global model which, in context of hyperspectral images, exploits spectral correlation whereas total variation is a local model which exploits spatial correlation within a band. The proposed spatio-spectral total variation (SSTV) model extends the traditional total variation model and accounts for both spatial and spectral correlation. The resulting optimization problem has been solved using split-Bregman approach [11]. We have compared our technique with three existing approaches namely LRMR [1], PCAW [4], and GSP [12]. We have also compared our technique by extending traditional hyperspectral total variation (HTV) model which considers sparse noise in addition to Gaussian noise. Peak signal to noise ratio (PSNR) and structural similarity index (SSIM) [13] are used to quantify the denoising results. Experimental results indicate that our proposed method is about 6.5 dB better in PSNR and 8% better in SSIM compared to existing technique [12] for a mixture of Gaussian and sparse noise.

Section II describes problem formulation followed by section III where we discuss the technique to solve proposed formulation. Section IV describes experimental results and section V concludes the paper with some future directions.

II. Problem Formulation

Define $y = \mathrm{vec}(Y)$ as vector representation of any 2D matrix obtained by vertical stacking of columns of matrix Y and $X = \mathrm{mat}(x)$ as its reverse operation. We use small letters for vectors and capital letters for matrices. A hyperspectral data cube of dimension $m \times n \times d$ having d spectral bands can be represented as $X = \begin{bmatrix} x_1 & x_2 & \dots & x_d \end{bmatrix}$ where each $x_i \in \mathbb{R}^{mn \times 1}$ $(mn = m \times n)$ is a spectral band obtained by vertical concatenation. Using these notations, image acquisition model in the presence of Gaussian and sparse noise can be expressed as:

$$Y = X + S + G,$$

where $X \in \mathbb{R}^{mn \times d}$ is original image, Y is noise corrupted image, S is sparse noise, and G is Gaussian noise. This model was introduced in [14] for low-rank matrix recovery problem and later utilized for hyperspectral denoising in LRMR algorithm [1].

The joint spatio-spectral correlation can be exploited by using synthesis prior approach or analysis prior approach. Synthesis prior approach seeks for sparse coefficients in a sparsifying transform domain. Let Z be the sparse representation of image X such that $Z = D_1 X D_2$. Here D_1 is a 2D sparsifying transform applied along spatial dimension, and D_2 is 1D sparsifying transform applied on spectral dimension. Using

Hemant Kumar Aggarwal and Angshul Majumdar are associated with Indraprastha Institute of Information Technology-Delhi, India. Hemant Kumar Aggarwal is supported by TCS research fellowship.

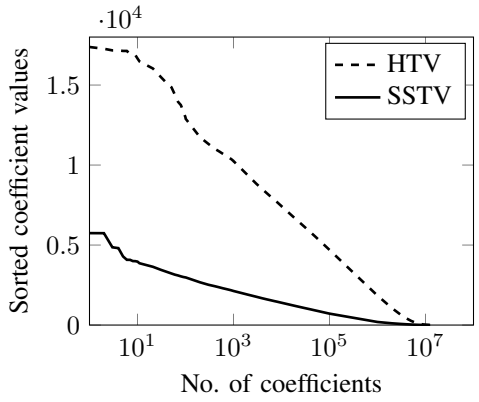

Fig. 1. Comparison of HTV model and proposed SSTV model.

these notations, general synthesis prior (GSP) formulation for mixed denoising problem can be expressed as:

$$\min_{Z,S} \|Z\|_1 + \|S\|_1 + \lambda \|Y - D_1^T Z D_2^T - S\|_F^2,$$

a solution to this problem is proposed by the authors in [12].

The pixels in most natural images are spatially correlated to its neighboring pixel values. The neighboring bands also exhibit high spectral correlation. This prior knowledge can be exploited by representing images as piece-wise smooth functions and can be modeled using total-variation regularization. The total variation for a gray scale image x can be expressed as

$$\mathrm{TV}(x) = \|D_h x\|_1 + \|D_v x\|_1$$

where D_h and D_v are horizontal and vertical 2D-finite differencing operators. This gray scale total variation model has been extended as CTV model in [15] for color images. This CTV model can be extended for a hyperspectral image X with d bands as follows:

$$\mathrm{HTV}(X) = \sum_{i=1}^{d} TV(x_i). \tag{1}$$

The denoising problem using HTV model can be expressed as:

$$\min_{X,S} \|Y - X - S\|_F^2 + \lambda \|S\|_1 + \mu\, \mathrm{HTV}(X) \tag{2}$$

This HTV model based hyperspectral denoising problem accounts for spatial correlation but does not consider spectral correlation present in neighboring bands of a hyperspectral image. We propose a spatio-spectral total variation model as follows:

$$\mathrm{SSTV}(X) = \|D_h X D\|_1 + \|D_v X D\|_1 \tag{3}$$

where $D \in \mathbb{R}^{b \times b}$ is one-dimensional finite differencing operator applied on spectral signature of each pixel such that discrete gradient at i^{th} pixel is $\alpha_i = (D^T z)_i = z_{i+1} - z_i$, where z represents spectral signature of a pixel and $\alpha \in \mathbb{R}^{b \times 1}$ with $\alpha_b = 0$ at boundary. This model simultaneously explores correlation in both spatial and spectral dimension. Figure 1 show the comparison of SSTV model with HTV model when applied on WDC hyperspectral image (data described in section 4). We observe that sorted discrete gradient coefficients for SSTV model give sparser representation compared to HTV model because SSTV model also exploits spectral correlation. The denoising problem using this SSTV model can be expressed as :

$$\min_{X,S} \|Y - X - S\|_F^2 + \lambda \|S\|_1 + \mu\, \mathrm{SSTV}(X) \tag{4}$$

where λ, μ are regularization parameters. Here ℓ_1-norm of S is minimized since S is representing sparse noise. Here $G = Y - X - G$ is representing Gaussian noise and therefore we are minimizing Frobenius norm of $Y - X - S$ to reduce variance of Gaussian noise.

Other studies in hyperspectral denoising has also used total variation based formulation such as [16]. However our study is markedly different from the aforesaid work in terms of noise model as well as total variation model.

Although researchers have proposed generic noise removal techniques [1], [4]; such an explicit formulation for jointly denoising Gaussian and sparse noise using spatio-spectral total variation has not been attempted before. We are not aware of any efficient algorithm that can solve the aforesaid problem. Therefore in the next section we describe how to solve this problem using split-Bregman [11] based approach.

III. Proposed Algorithm

The problem formulation (4) can be expressed as :

$$\min_{X,S} \|Y - X - S\|_F^2 + \lambda \|S\|_1 + \mu \|D_h X D\|_1 + \mu \|D_v X D\|_1$$

This is a high-dimensional non-differentiable optimization problem in X and S. Since the variable X is not separable, we can re-write it into constrained formulation :

$$\begin{aligned} \underset{X,S}{\text{minimize}} \quad & \|Y - X - S\|_F^2 + \lambda \|S\|_1 + \mu \|P\|_1 + \mu \|Q\|_1 \\ \text{subject to} \quad & P = D_h X D \\ & Q = D_v X D \end{aligned}$$

The above constrained optimization problem can be expressed as unconstrained optimization problem using quadratic penalty function as follows:

$$\begin{aligned} \underset{P,Q,X,S}{\text{minimize}} \; & \|Y - X - S\|_F^2 + \lambda \|S\|_1 + \mu \|P\|_1 + \mu \|Q\|_1 \\ & + \nu \|P - D_h X D\|_F^2 + \nu \|Q - D_v X D\|_F^2 \end{aligned}$$

where ν is regularization parameter. The same parameter ν is used for both horizontal and vertical total variation regularization terms for considering their equal contributions. However the above problem is in four variables (P, Q, X, S) but it is now separable. Since there are multiple regularization terms, we intent to follow the split-Bregman [11] approach which can be applied to solve this problem. By using Bregman variables B_1, and B_2, we can rewrite the problem as:

$$\begin{aligned} \underset{P,Q,X,S}{\text{minimize}} \; & \|Y - X - S\|_1^2 + \lambda |S\|_1 + \mu \|P\|_1 + \mu \|Q\|_1 \\ & + \nu \|P - D_h X D - B_1\|_F^2 + \nu \|Q - D_v X D - B_2\|_F^2 \end{aligned}$$

The above problem can be split into following relatively easy to solve four sub-problems:

$$\begin{aligned}
\text{P1}: &\quad \min_{P}\ \mu\|P\|_1 + \nu\|P - D_h X D - B_1\|_F^2 \\
\text{P2}: &\quad \min_{Q}\ \mu\|Q\|_1 + \nu\|P - D_v X D - B_2\|_F^2 \\
\text{P3}: &\quad \min_{S}\ \lambda\|S\|_1 + \|Y - X - S\|_F^2 \\
\text{P4}: &\quad \min_{X}\ \|Y - X - S\|_F^2 + \nu\|P - D_h X D - B_1\|_F^2 \\
&\qquad + \nu\|Q - D_v X D - B_2\|_F^2
\end{aligned}$$

The sub-problems P1, P2, and P3 are of the form :

$$\arg\min_{X} \|Y - X\|_F^2 + \alpha\|X\|_1$$

which can be solved by using soft-thresholding [17] operation:

$$\hat{X} = \text{SoftTh}(Y, \alpha) = \text{sign}(Y) \times \max\left\{0, |Y| - \frac{\alpha}{2}\right\},$$

Sub-problem P4 is a least-square problem but variable X is not de-coupled. Let $\nabla_h = D^T \otimes D_h$, $\nabla_v = D^T \otimes D_v$. We can rewrite the problem P4 as:

$$\min_{x} \|y - x - s\|_2^2 + \nu\|p - \nabla_h x - b_1\|_2^2 + \nu\|q - \nabla_v x - b_2\|_2^2$$

Here we have used the property of Kronecker product that $A = BCD$ can be expressed as $a = (D^T \otimes B)c$. Here small letters represents vector form of corresponding matrix. After differentiating, we get following linear system of equations:

$$(I + \nu\nabla)x = \mu(y - s) + \nu\nabla_h^T(p - b_1) + \nu\nabla_v^T(q - b_2) \quad (5)$$

with $\nabla = \nabla_h^T\nabla_h + \nabla_v^T\nabla_v$. This problem can be solved using iterative least square solvers such as LSQR [18]. Bregman variables B_1, B_2 can be updated in each iterations (k) as follows:

$$\begin{aligned}
B_1^{k+1} &= B_1^k + D_h X D - P \\
B_2^{k+1} &= B_2^k + D_v X D - Q
\end{aligned}$$

Algorithm 1 summaries the steps of proposed spatio-spectral total variation (SSTV) algorithm.

Algorithm 1 Spatio-Spectral Total Variation Algorithm

input: Y, λ μ, ν, MaxIter
output: $\hat{X}$ (denoised image).
for $k = 1$ to MaxIter **do**
  $P^{k+1} = \text{SoftTh}(D_h X^k D + B_1^k, \frac{\mu}{\nu})$
  $Q^{k+1} = \text{SoftTh}(D_v X^k D + B_2^k, \frac{\mu}{\nu})$
  $S^{k+1} = \text{SoftTh}(Y - X^k, \lambda)$
  $X^{k+1} = \text{mat}(x)$ from (5)
  $B_1^{k+1} = B_1^k + D_h X^{k+1} D - P^{k+1}$
  $B_2^{k+1} = B_2^k + D_v X^{k+1} D - Q^{k+1}$
end for
return $\hat{X} = X^{k+1}$

IV. Experiments and Results

Experiments were performed with two hyperspectral image datasets. The first dataset is of Washington DC (WDC) mall [19] from Hyperspectral Digital Imagery Collection Experiment (HYDICE) sensor having $1m$ spatial resolution and 10-nm band spacing covering spectral range of 400-2500 nm. We considered a patch of size $256 \times 256 \times 190$ from *WDC* image for experiments. Second image was of Gulf of Mexico area [20] from SpecTIR having $2m$-spatial resolution and 5-nm band spacing covering spectral range of 395-2450-nm. A patch of size $256 \times 256 \times 160$ was considered for performing experiments.

The proposed algorithm SSTV was compared with four existing denoising algorithms LRMR [1], PCAW [4], GSP [12], and HTV. The LRMR [1] approach is based on a low rank matrix recovery algorithm [21]. It explores low-rank nature of a hyperspectral image for denoising. The PCAW [4] approach is a principle component analysis based (PCA) approach which keeps initial high energy PCA components unaltered and then perform wavelet-thresholding on low energy components along both spatial and spectral dimension. The GSP [12] algorithm is a general synthesis prior algorithm which also explicitly consider sparse noise in the problem formulation. It explores sparsity of the hyperspectral data cube along both spatial and spectral dimensions. HTV algorithm is based on band-by-band total variation model which also consider sparse noise. We can obtain HTV algorithm by setting 1D total variation operator D to identity operator in Algorithm 1.

All the unknown variables (X, S, P, Q, B_1, B_2) required by our algorithm were initialized to zero. All three parameter values $\lambda = 0.1,\ \mu = 0.2,\ \nu = 0.2$ were found empirically. Although our proposed algorithm (SSTV) depends on three regularization parameters (λ, μ, ν) but the algorithm is not very sensitive to the specific values of these parameters and allows a broad range of values. These parameters can be adjusted to get desired denoising strength however we had kept the parameter values constant for all the synthetic as well as real data experiments. The value of parameter λ adjusts the denoising strength corresponding to sparse noise whereas parameters μ and ν provides trade off between retaining original image and smoothness by total-variation regularization respectively.

Parameters for the LRMR algorithm (rank=4 and sparsity=4000) were set to yield the best results as described in the paper [1]. We utilized 3D-DCT as sparsifying transform in the general synthesis prior (GSP) algorithm i.e. $2D$-DCT to sparsify each spectral band image and 1D-DCT to sparsify across the spectral bands. The first five high energy PCA components were kept unaltered in the PCAW algorithm and wavelet shrinkage was applied with a window size of 1×3 as described in the paper [4]. The parameter value of $\lambda = 1,\ \mu = .5,\ \nu = 0.01$ were empirically found to give best results on both the hyperspectral datasets in HTV algorithm.

The first set of experiments were conducted to experimentally check the convergence of proposed algorithm. Figure 2 shows the variation of objective function (4) value with number of iterations. It can be observed that after 40 iterations objective function value converges to a locally optimal value.

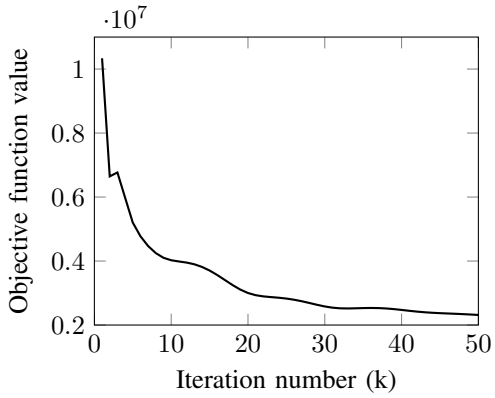

Fig. 2. Convergence of proposed SSTV algorithm

Therefore we can stop our algorithm after 40 iterations.

The second set of experiments were conducted with synthetic noise so as to check the robustness of proposed method with respect to different noise levels. The denoising results are quantified using peak signal to noise ration (PSNR) and structural similarity index (SSIM). PSNR between original image X and reconstructed image Y was calculated as:

$$\mathrm{PSNR} = \frac{1}{d}\sum_{i=1}^{d} 10\log_{10}\left(\frac{\max(x_i)^2}{\mathrm{MSE(x_i, y_i)}}\right)$$

where $\mathrm{MSE}(x_i, y_i)$ represents mean square error between bands x_i and y_i. Structural similarity index takes into account hue, contrast and shape of restored image and gives a normalized score between zero and one where maximum value of one represents a perfect match. Table I summarizes the comparison of PSNR (dB) and SSIM values obtained from different experiments. Maximum value of PSNR and SSIM values for each experiment is bold faced. It can be observed from Table I that proposed SSTV algorithm have high PSNR and SSIM values when all four kinds of noise are present in the hyperspectral image. The HTV algorithm does not consider spectral information therefore PSNR and SSIM values are comparatively lower for this algorithm.

Figure 3 visually compares the denoising results on band 110 of WDC image when all four kinds of noise are present. Figure 3(a) shows original Band 110 of WDC image. All bands were corrupted by synthetically added Gaussian noise of SNR=20 and 5% impulse noise. Band number $60, 110, 111, 132$ were corrupted by four deadlines and line strips. Horizontal deadlines were located at $30, 100, 112, 220$ and vertical deadlines were located at $70, 118, 128, 220$. This mixed noise corrupted image is shown in Fig. 3(b). Both HTV and PCAW methods are able to reduce Gaussian noise and some impulse noise as observed in Fig. 3(c) and 3(d). Both of these methods are not able to reduce either deadlines or line strips. LRMR method is able to reduce all these four kinds of noise but still some noise can be visualized in reconstructed image 3(e). It can be observed from Fig. 3(f) and 3(g) that visual quality of denoised images by GSP method and proposed SSTV method is better than other methods compared against however GSP results look somewhat over-smooth.

The third set of experiments were conducted with real noisy hyperspectral images. Denoising results obtained by different algorithms are shown in Fig. 4. Several bands of the Gulf image have noise. Figure 4(a) shows original band 120 of Gulf image which is a noisy band. HTV method (Fig. 4(b)) and LRMR method (Fig. 4(d)) have reduced noise but some noise is still visible. PCAW (Fig. 4(c)) method is not able to reduce noise from this image. The zoomed portions of images displayed in Fig. 4(e) and 4(f) clearly shows that different kinds of noise have been effectively reduced by both GSP and proposed SSTV methods.

V. Conclusions

In this work, we have proposed a mixed noise reduction algorithm based on spatio-spectral total variation regularization. A general noise model has been considered which accounts for not only Gaussian noise but also sparse noise. Inherent structure of hyperspectral images has been explored by utilizing $2D$ total-variation along spatial dimension and 1D total-variation along spectral dimension. The denoising problem has been formulated as an optimization problem whose solution has been derived using split-Bregman approach. Experimental results demonstrates that proposed algorithm is able to reduce significant amount of noise from real noisy hyperspectral images compared to existing state of art approaches.

Our Matlab implementation of proposed algorithms is available from [22] for the sake of reproducible research.

References

[1] H. Zhang, W. He, L. Zhang, H. Shen, and Q. Yuan, "Hyperspectral Image Restoration Using Low-Rank Matrix Recovery," *IEEE Trans. Geosci. Remote Sens.*, vol. 52, no. 8, pp. 4729–4743, 2014.

[2] P. Liu, F. Huang, G. Li, and Z. Liu, "Remote-Sensing Image Denoising Using Partial Differential Equations and Auxiliary Images as Priors," *IEEE Geosci. Remote Sens. Lett.*, vol. 9, no. 3, pp. 358–362, 2012.

[3] X. Liu, S. Bourennane, and C. Fossati, "Nonwhite Noise Reduction in Hyperspectral Images," *IEEE Geosci. Remote Sens. Lett.*, vol. 9, no. 3, pp. 368–372, 2012.

[4] G. Chen and S.-E. Qian, "Denoising of Hyperspectral Imagery Using Principal Component Analysis and Wavelet Shrinkage," *IEEE Trans. Geosci. Remote Sens.*, vol. 49, no. 3, pp. 973–980, 2011.

[5] X. Liu, S. Bourennane, and C. Fossati, "Denoising of Hyperspectral Images Using the PARAFAC Model and Statistical Performance Analysis," *IEEE Trans. Geosci. Remote Sens.*, vol. 50, no. 10, pp. 3717–3724, 2012.

[6] J. Xu, W. Wang, J. Gao, and W. Chen, "Monochromatic Noise Removal via Sparsity-Enabled Signal Decomposition Method," *IEEE Geosci. Remote Sens. Lett.*, vol. 10, no. 3, pp. 533–537, 2013.

[7] D. Cerra, M. Rupert, and P. Reinartz, "Noise Reduction in Hyperspectral Images Through Spectral Unmixing," *IEEE Geosci. Remote Sens. Lett.*, vol. 11, no. 1, pp. 109–113, 2014.

[8] M. Yan, "Restoration of Images Corrupted by Impulse Noise and Mixed Gaussian Impulse Noise Using Blind Inpainting," *SIAM J. Imaging Sci.*, vol. 6, no. 3, pp. 1227–1245, 2013.

[9] Y. Xiao, T. Zeng, J. Yu, and M. K. Ng, "Restoration of images corrupted by mixed Gaussian-impulse noise via l1-l0 minimization," *Pattern Recognit.*, vol. 44, no. 8, pp. 1708–1720, 2011.

[10] J. Liu, X.-C. Tai, H. Huang, and Z. Huan, "A weighted dictionary learning model for denoising images corrupted by mixed noise." *IEEE Trans. Image Process.*, vol. 22, no. 3, pp. 1108–20, 2013.

[11] T. Goldstein and S. Osher, "The Split Bregman Method for L1-Regularized Problems," *SIAM J. Imaging Sci.*, vol. 2, no. 2, pp. 323–343, 2009.

[12] H. K. Aggarwal and A. Majumdar, "Mixed Gaussina and Impulse Denoising of Hyperspectral Images," in *IEEE Geosci. Remote Sens. Symp.*, 2015, pp. 429–432.

TABLE I
COMPARISON OF PSNR AND SSIM VALUES OBTAINED BY DIFFERENT ALGORITHMS FOR DIFFERENT KINDS OF MIXED NOISE.

Mixed noise	Peak Signal to Noise Ratio (dB)						Structural Similarity Index					
	Noisy	HTV	PCAW	LRMR	GSP	SSTV	Noisy	HTV	PCAW	LRMR	GSP	SSTV
Gaussian(SNR=20)	30.29	35.18	40.44	39.98	36.86	**41.12**	0.90	0.93	**0.99**	0.98	0.97	**0.99**
Gaussian(SNR=20) + impulse(5%)	17.01	25.84	30.81	35.12	33.55	**40.38**	0.52	0.78	0.90	0.97	0.95	**0.98**
Gaussian(SNR=20) + impulse(10%) + 4 horizontal & 4 vertical lines	14.17	21.14	25.99	27.59	32.96	**39.88**	0.33	0.59	0.83	0.87	0.94	**0.98**

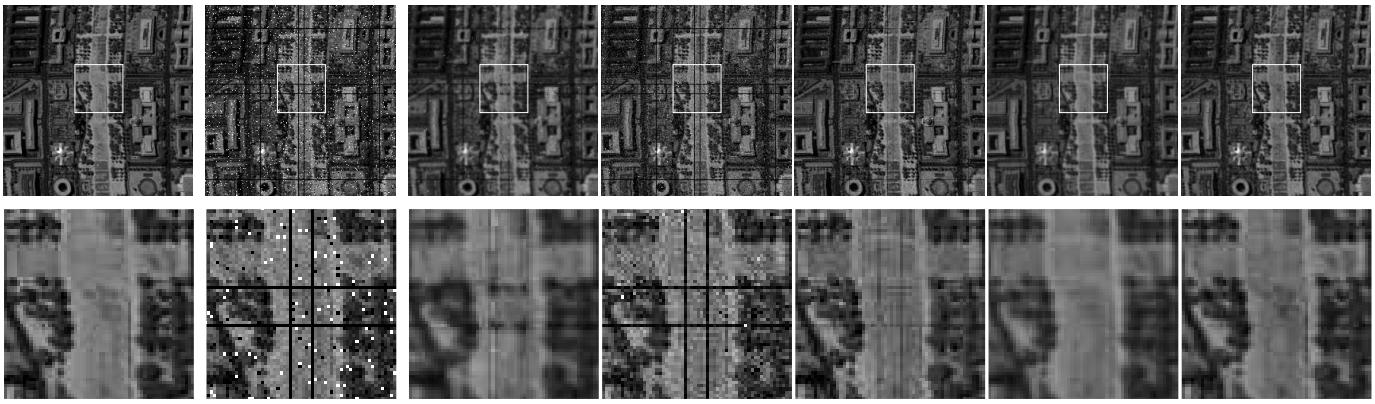

(a) Original (b) Noisy (c) HTV (d) PCAW (e) LRMR (f) GSP (g) Proposed

Fig. 3. Comparison of visual quality of denoising results with synthetic noise in WDC hyperspectral image by different algorithms. Top row: Band 110 denoised by various algorithms. Bottom row: zoomed in portion of the same band marked with white square.

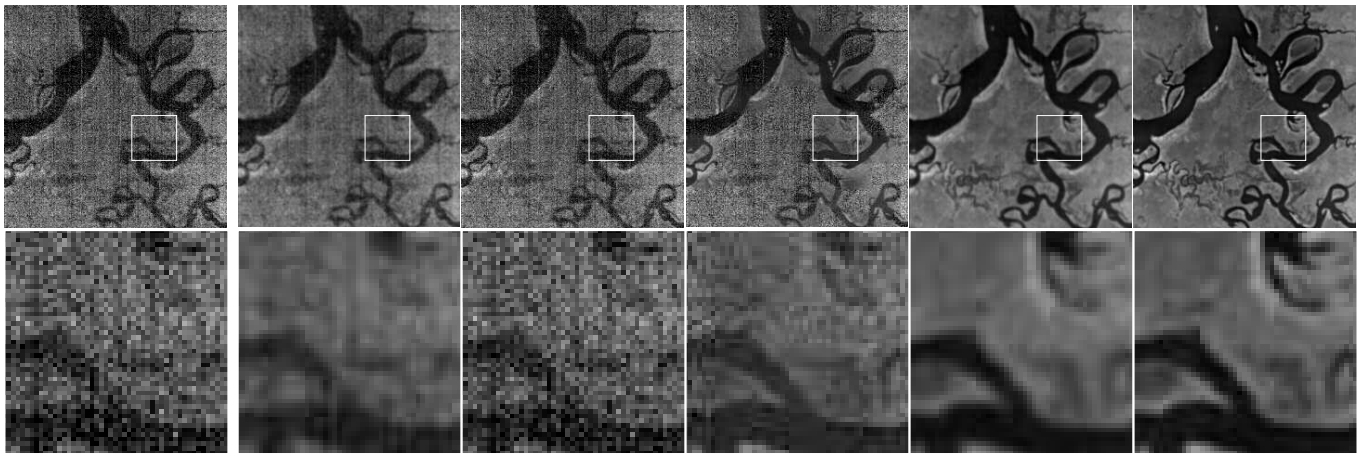

(a) Original (b) HTV (c) PCAW (d) LRMR (e) GSP (f) Proposed

Fig. 4. Comparison of visual quality of denoising results on real noisy Gulf hyperspectral image by different algorithms. Top row: Band 120 denoised by various algorithms. Bottom row: zoomed in portion of the same band.

[13] Z. Wang, A. C. Bovik, H. R. Sheikh, and E. P. Simoncelli, "Image quality assessment: from error visibility to structural similarity." *IEEE Trans. Image Process.*, vol. 13, no. 4, pp. 600–12, 2004.

[14] Z. Zhou, X. Li, J. Wright, E. Candes, and Y. Ma, "Stable principal component pursuit," in *IEEE International Symposium on Information Theory*. IEEE, 2010, pp. 1518–1522.

[15] P. Blomgren and T. F. Chan, "Color TV: total variation methods for restoration of vector-valued images." *IEEE Trans. Image Process.*, vol. 7, no. 3, pp. 304–9, 1998.

[16] Q. Yuan, L. Zhang, and H. Shen, "Hyperspectral Image Denoising Employing a Spectral Spatial Adaptive Total Variation Model," *IEEE Trans. Geosci. Remote Sens.*, vol. 50, no. 10, pp. 3660–3677, 2012.

[17] M. A. T. Figueiredo and R. D. Nowak, "An EM Algorithm for Wavelet-Based Image Restoration," *IEEE Trans. Image Process.*, vol. 12, no. 8, pp. 906–916, 2003.

[18] M. A. Saunders, "Solution of Sparse Rectangular Systems Using LSQR and CRAIG," *BIT Numer. Math.*, vol. 35, no. 4, pp. 588–604, 1995.

[19] WDC, "Dataset, last accessed: 20-Jan-2015," https://engineering.purdue.edu/%7ebiehl/MultiSpec/hyperspectral.html.

[20] G. of Mexico, "Dataset, last accessed : 20-Jan-2015," http://www.spectir.com/free-data-samples/.

[21] T. Zhou and D. Tao, "GoDec : Randomized Low-rank and Sparse Matrix Decomposition in Noisy Case," in *Int. Conf. Mach. Learn.*, 2011, pp. 33–40.

[22] H. K. Aggarwal, "Mixed Noise Reduction," http://www.mathworks.com/matlabcentral/fileexchange/49145-mixed-noise-reduction, 2015.